Analyst

ROYAL SOCIETY OF CHEMISTRY

CRITICAL REVIEW

Published on 25 June 2026

Cite this: DOI: 10.1039/d6an00535g

Analytical challenges in mapping the subcellular metabolome and lipidome

Marta Nobile, [a] Simone Serrao,[a] Eleonora Bossi,[a] Francesca Re, [a,b] Francesca Raimondo[a] and Giuseppe Paglia *[a]

Received 8th May 2026,
Accepted 24th June 2026

DOI: 10.1039/d6an00535g

rsc.li/analyst

Mass spectrometry-based metabolomics and lipidomics are central analytical tools for characterizing cellular chemical composition. However, most workflows still rely on the simplifying assumption of homogeneous intracellular pools, which is increasingly inadequate for spatially organized eukaryotic systems. Metabolites and lipids are distributed across subcellular compartments that differ in chemical environment, turnover, and accessibility, thereby affecting both measurement and interpretation. Recent advances in subcellular and spatial metabolomics have highlighted both the potential and the limitations of organelle-resolved analysis, particularly in terms of extraction chemistry, quantification, and data interpretation. In this review, we critically examine organelle-resolved metabolomics and lipidomics from a mass spectrometry–centric perspective, treating subcellular compartmentalization as an analytical variable rather than solely a biological feature. By comparing metabolomics and lipidomics studies on subcellular compartments, we evaluate fractionation-based, affinity-based, and spatial MS strategies, and we highlight current capabilities, common artefacts, and future opportunities, including the integration of stable isotope tracing and emerging single-organelle approaches such as Nanoscale Secondary Ion Mass Spectrometry (NanoSIMS) and Direct Organelle Mass Spectrometry (DOMS).

1. Introduction

Mass spectrometry (MS)-based metabolomics and lipidomics have established themselves as powerful analytical platforms in translational and preclinical research. These techniques enable the simultaneous profiling of thousands of small-molecule metabolites and lipids in complex biological matrices, including biofluids (plasma, urine), tissues, cells, and minimally invasive samples such as dried blood spots (DBS).[1–6] Liquid chromatography and gas chromatography coupled to MS (LC-MS and GC-MS, respectively) platforms provide high sensitivity and coverage, enabling the detection of slight metabolic perturbations at early, often pre-symptomatic, stages of disease while facilitating biomarker discovery. By profiling downstream cellular products, these approaches bridge genomics, proteomics, and phenotype, revealing real-time metabolic remodeling in conditions such as cancer, cardiovascular diseases, diabetes, and neurodegeneration.[7–13]

By identifying dysregulated pathways, metabolomics has also become central to precision and personalized medicine, supporting early detection, patient stratification based on individual metabolic phenotypes, treatment response monitoring, and accelerated drug development. However, a fundamental limitation remains largely overlooked. Most workflows treat the intracellular space as a homogeneous, well-mixed system. As a result, classical bulk extraction collapses chemically distinct intracellular pools into a single composite signal, masking compartment-specific biology.

However, in eukaryotic cells metabolism and lipid biology are intrinsically compartmentalized: organelles operate as specialized biochemical hubs with distinct enzymatic activities, chemical environments (pH, redox state, enzyme density), and transport mechanisms, which are essential for cellular homeostasis.[14] For example, processes such as mitochondrial oxidative phosphorylation and lysosomal degradation exemplify this spatial organization,[15] leading to spatially segregated pools of the same molecular species across compartments.

Lipids, in particular, serve as the structural backbone of this compartmentalization, with their composition and distribution defining organelle identity and function.[16] As a result, whole-cell metabolomics yields averaged signals that can obscure localized biochemical alterations, despite its value for broad molecular coverage and biomarker discovery.

In pathological conditions, opposing changes in different compartments may cancel each other out at the bulk level, leading to underestimation or misinterpretation of disease-related processes. Therefore, understanding disease requires

[a]School of Medicine and Surgery, University of Milano-Bicocca, Via Raoul Follereau 3, 20854 Vedano al Lambro, MB, Italy. E-mail: giuseppe.paglia@unimib.it
[b]Fondazione IRCCS San Gerardo dei Tintori, Via Pergolesi 33, 20900 Monza, MB, Italy

not only quantitative information but also spatial context, particularly in metabolic and neurodegenerative disorders, where the sequestration of metabolites within specific organelles like mitochondria or lysosomes often defines the pathological state.[17,18]

To provide a first-order view of how unevenly subcellular information is currently represented in reference databases, we interrogated the Human Metabolome Database (HMDB, version 5.0, released 2022, accessed April 2026),[19] which currently includes 119 481 annotated metabolites. These entries include detected and quantified, detected but not quantified, and expected but not yet experimentally confirmed metabolites. Among these, only a limited subset (n = 8209; ~6.9%) is associated with expert-curated subcellular localization information, highlighting a substantial knowledge gap in spatial metabolomics.

Within the localized metabolome, the cytosol represents the predominant compartment (n = 7819), consistent with its role as the central hub of primary metabolism. This compartment is dominated by highly abundant, soluble intermediates, including sugars (*e.g.*, glucose), amino acids (*e.g.*, glutamate), and key glycolytic metabolites such as pyruvate and lactate. In contrast, a markedly smaller fraction of metabolites is associated with mitochondria (n = 310), where the metabolome is enriched in tricarboxylic acid (TCA) cycle intermediates (*e.g.*, citrate, succinate) and redox cofactors (*e.g.*, NADH), reflecting the specialized role of this organelle in energy metabolism. The nuclear metabolome (n = 80) is even more restricted and is enriched in metabolites involved in regulatory processes, such as nucleotides (*e.g.*, CMP, dUMP) and methyl donors (*e.g.*, *S*-adenosylmethionine), which are essential for epigenetic modifications and transcriptional control (Fig. 1 and SI Table S1).

This imbalance likely reflects both biological factors and annotation bias: abundant, central metabolites and well-studied pathways are more likely to be localized than low-abundance, transient, or poorly characterized species. Therefore, this distribution should be interpreted as a reflection of current knowledge representation rather than a quantitative estimate of the true intracellular metabolome.

The situation is even more constrained for lipids. LIPID MAPS (accessed March 2026)[20,21] is primarily a structure- and classification-centered resource that provides expert-curated lipid records, cross-references, and annotations. While it is indispensable for lipid nomenclature, classification, and structural annotation, it is not a comprehensive molecule-by-molecule database of experimentally validated subcellular localization. It provides an extensive catalog of over 60 000 lipid structures, yet subcellular localization is available only for a limited subset of entries. Lipid compartmentalization is inferred on the basis of established biosynthetic pathways, membrane composition, and repeatedly observed organelle-enrichment patterns from the literature, rather than presented as an exhaustive localization census derived directly from the database.

From this perspective, some broad principles are well supported: cardiolipin is strongly associated with mitochondria, sphingolipids are enriched in the plasma membrane and Golgi/endolysosomalsystem, and neutral lipids such as triacylglycerols and cholesteryl esters accumulate in lipid droplets. However, these represent class-level localization trends rather than comprehensive, molecule-specific assignments.

Despite these limitations, integration of pathway knowledge with available localization counts allows an overview of lipid compartmentalization. Out of 62 808 lipids annotated in LIPID MAPS, approximately 52 889 can be assigned to at least one subcellular compartment based on current annotations and inferences (Fig. 2 and SI Table S2).

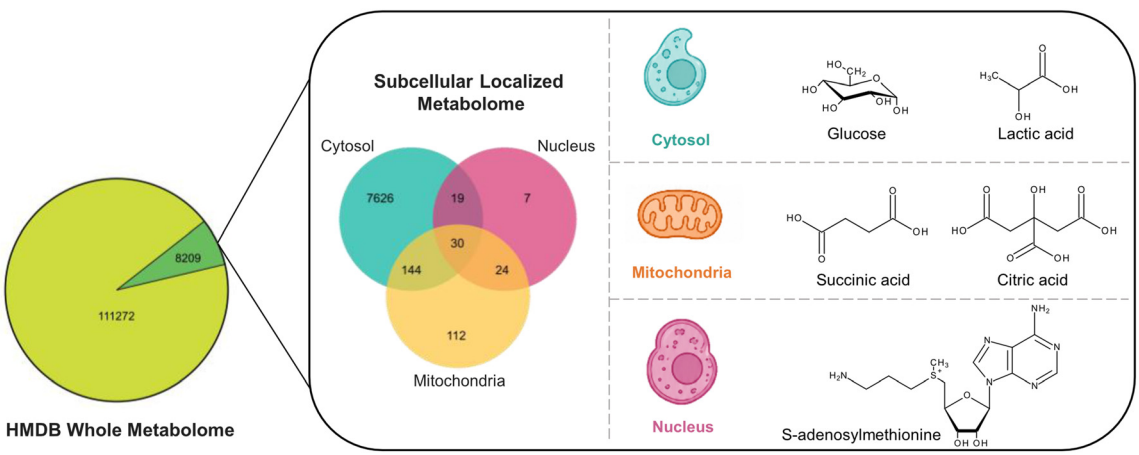

Fig. 1 Overview of metabolite distribution across major subcellular compartments. The figure combines a pie chart summarizing the fraction of metabolites with and without subcellular annotation in the Human Metabolome Database (HMDB) with a Venn diagram illustrating the overlap and compartment-specific distribution of annotated metabolites across the cytosol, nucleus, and mitochondria. Representative metabolites and their chemical structures associated with each organelle are also reported to highlight characteristic compartment-specific metabolic features. The pie chart emphasizes the still limited proportion of metabolites currently assigned to defined intracellular localizations, while the Venn diagram illustrates the relative overlap between major subcellular compartments [SI Table S1].

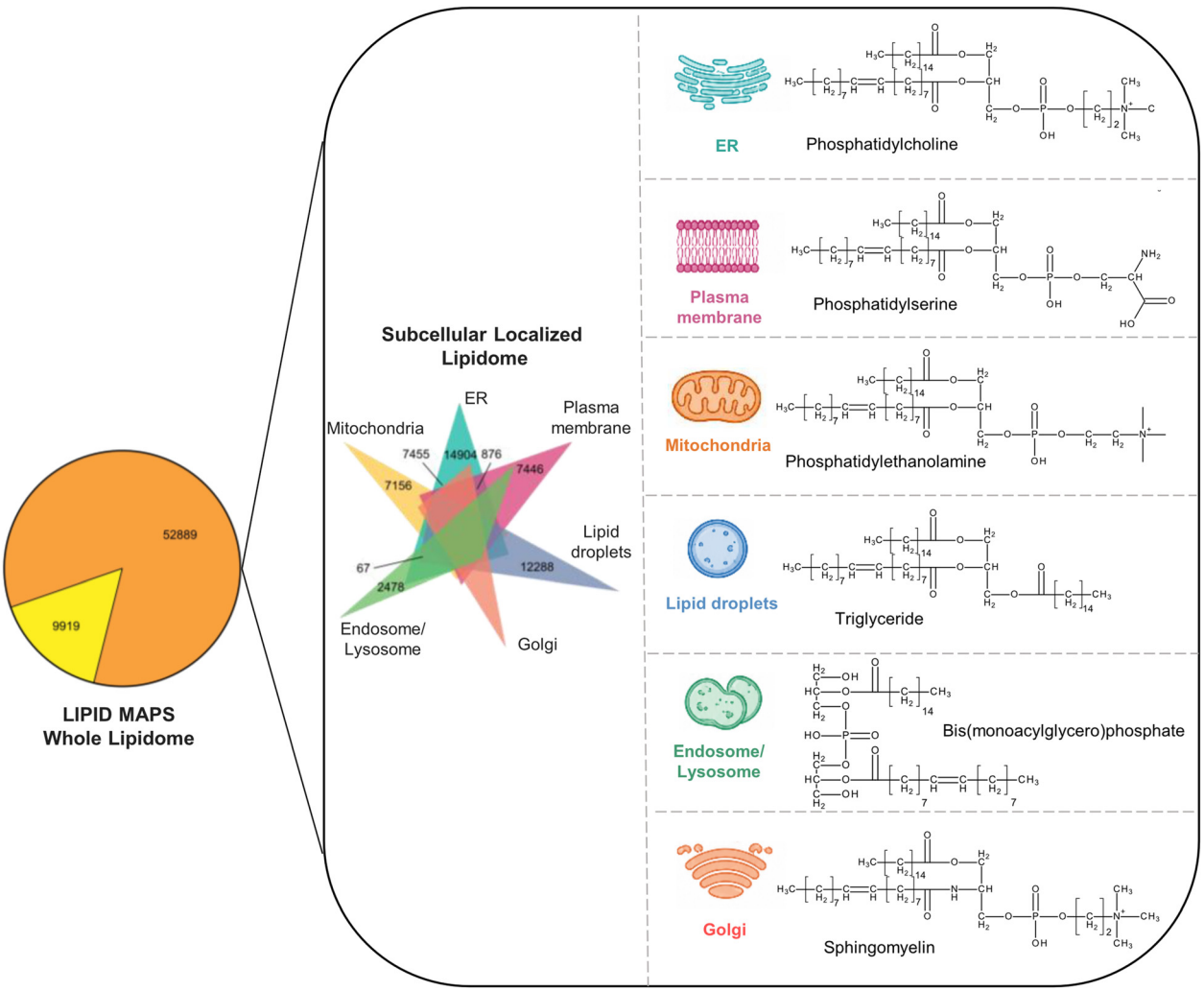

Fig. 2 Overview of lipid distribution across major subcellular compartments. The figure combines a pie chart summarizing the fraction of lipids with and without subcellular annotation in the LIPID MAPS database with a graphical representation illustrating the compartment-specific distribution of annotated lipids across major organelles, including the endoplasmic reticulum, plasma membrane, mitochondria, lipid droplets, endosome/lysosome, and Golgi apparatus. Representative lipid classes and their chemical structures associated with each compartment are also shown to highlight characteristic organelle-specific lipid compositions. The pie chart emphasizes the still limited proportion of lipids currently assigned to defined intracellular localizations, while the compartmental representation illustrates the heterogeneous distribution of lipid species across cellular organelles [SI Table S2].

Taken together, these database surveys highlight an important analytical and knowledge gap: subcellular localization remains incompletely annotated. Compartmentalization deserves greater attention in the metabolomics community, where it remains an underappreciated issue. It is not only a biological feature, but also a major analytical challenge that affects every stage of the workflow, from sampling and extraction to matrix effects, quantification, and data interpretation. This spatial distribution is particularly evident in lipid biology, where lipids play a structural role in defining organelle identity and function. Unlike small polar metabolites, which are highly soluble and can rapidly shuttle between compartments, most lipids are membrane-anchored or confined within specific lipid assemblies. This physical confinement generally makes organelle-resolved lipidomics more robust and less prone to leakage.

This review examines subcellular metabolomics and lipidomics from a mass spectrometry-centric perspective, with a focus on the analytical consequences of intracellular compartmentalization. Rather than treating organelle localization solely as a biological attribute, we consider it a variable that directly affects sampling, fractionation, extraction, ionization, quantification, and data interpretation. We argue that the analytical behavior of compartment-resolved metabolomics and lipidomics differs substantially, largely because small polar metabolites are highly dynamic and diffusible, whereas many lipids are structurally anchored to membranes and therefore more resistant to redistribution during isolation. By

comparing fractionation-based, affinity-based, and spatial MS approaches, we outline both the potential and the current limits of organelle-resolved analysis, and discuss how integration with isotope tracing and multi-omics may improve the interpretation of compartment-specific metabolism.

2. Compartmentalization as an analytical variable in cellular metabolomics and lipidomics

2.1 Bulk workflows measure composite intracellular pools

Bulk metabolomics and lipidomics analyses are built on several key assumptions that simplify data interpretation but are increasingly questioned in light of emerging subcellular and spatial studies. A primary assumption is that metabolites and lipids are homogeneously distributed, such that whole-cell extracts reflect the true biological state.[15,21–23] In reality, sequestration into organelles and membrane association generates spatially distinct pools that are averaged during bulk extraction. A second critical assumption concerns the technical integrity of the sample: effective quenching and maintenance of steady-state conditions are presumed to prevent post-collection changes, while sample preparation is expected to cause negligible redistribution. However, incomplete quenching often allows residual activity, particularly for highly labile compounds like nucleotides or redox-sensitive species.[24] Failure to rapidly arrest metabolism, combined with lysis and extraction, can induce leakage, exchange, and redistribution across compartments.

Recent evidence shows that such processes can disrupt *in vivo* gradients and alter pool compositions, especially for polar metabolites or amphiphilic lipids.[15] Finally, MS signals are often interpreted as direct proxies of intracellular concentrations, despite the influence of extraction efficiency, ionization bias, and matrix effects.[15]

While these assumptions enabled widespread adoption of bulk approaches, their limitations are increasingly evident in subcellular studies. The same molecular species can exist in chemically and kinetically distinct pools across compartments, resulting in composite signals that obscure functional differences.[3,15,22]

2.2 Subcellular chemical microenvironments and dynamic compartmentalization

Subcellular compartments do not merely serve as biological containers; they establish distinct chemical microenvironments that profoundly influence metabolite stability, reaction kinetics, and analytical outcomes. Mitochondria maintain a highly negative membrane potential, an alkaline matrix pH (~7.8–8.0), and a reducing redox environment (high NADH/NAD^+ and NADPH/$NADP^+$ ratios), favoring oxidative phosphorylation and ROS management.[25] Lysosomes exhibit an acidic pH (~4.5–5.0), oxidative redox conditions, and high hydrolytic enzyme density, optimized for degradation.[26] The cytosol is near-neutral (pH ~7.2), with a more balanced redox state and lower enzyme specialization for specific pathways.[27] The endoplasmic reticulum features a more oxidizing environment for protein folding and lipid synthesis,[28] peroxisomes harbor high catalase activity and oxidative conditions for fatty acid β-oxidation,[29] and the nucleus maintains a pH close to that of the cytosol but with unique ion and protein compositions influencing gene regulation.[30]

These differences create reaction environments that directly affect metabolite stability, extractability, and MS detectability.[16,31,32]

In addition, compartmentalization is highly dynamic. Metabolites continuously shuttle *via* transporters and vesicular trafficking, generating concentration gradients across membranes. Many reactions are spatially restricted (*e.g.*, TCA cycle in mitochondria), making bulk measurements insensitive to these dynamics. Quenching and extraction can further disrupt these gradients, posing a major analytical challenge.[15,24]

From an analytical perspective, compartments should be viewed not simply as biological labels, but as chemical microenvironments that shape metabolite stability, extractability, and MS detectability.

2.3 Origins of compartment-specific pools

Compartment-specific metabolite and lipid pools arise from several interconnected mechanisms that generate analytically distinct subpopulations, even for chemically identical molecular species.[33] First, physical separation and selective transport are foundational: organelle membranes function as semi-permeable barriers where specific transporters—such as the SLC family for polar metabolites and ABC transporters for lipids—tightly regulate entry and exit.[15,34] This active gating creates steep concentration gradients and asymmetric distributions that are essential for cellular homeostasis, yet these gradients rapidly collapse during the cell lysis typical of bulk extraction workflows.

Second, membrane association and phase partitioning drive molecular enrichment based on physico-chemical properties such as hydrophobicity, surface charge, and lipid packing. This is particularly evident in hepatic lipid trafficking, where physical membrane-contact sites between lipid droplets and organelles enable the targeted partitioning of fatty acids, preventing their unregulated dispersion into the cytosol.[35–37]

Finally, local enzyme enrichment and metabolic channeling add a layer of kinetic complexity. Enzymes often assemble into multi-enzyme complexes (metabolons) or anchor at membrane interfaces to funnel substrates directly from one active site to the next.[38] This 'kinetic isolation' produces metabolite pools with unique turnover rates and flux dynamics that do not equilibrate with the rest of the cell.

Together, these mechanisms generate chemically and kinetically distinct pools that collapse into composite signals upon bulk extraction, obscuring spatial information.[39] This loss of spatial and kinetic context represents one of the central analytical limitations of bulk MS-based metabolomics and lipidomics.

3. Experimental strategies for organelle-resolved metabolomics and lipidomics

Because compartment-specific pools are chemically fragile and often operationally inaccessible, any isolation strategy inevitably involves a trade-off between spatial specificity and molecular preservation. Current strategies broadly fall into two categories: fractionation-based methods, which physically separate organelles before MS analysis, and *in situ* spatial methods, which aim to preserve the native cellular architecture. Each approach presents distinct advantages and limitations in spatial resolution, chemical coverage, throughput, and quantitative reliability.

3.1 Fractionation for organelles isolation methods

Every fractionation workflow begins with organelle release, consisting of the controlled disruption of the plasma membrane to obtain intact organelles. Typical approaches include mechanical homogenization using a Dounce or Potter-Elvehjem homogenizer, brief sonication, osmotic shock, or mild detergent-based permeabilization. The choice of method is critical: insufficient disruption reduces yield, whereas excessive force induces leakage and degradation of labile metabolites and lipids.[40,41] The selection of an appropriate lysis buffer is a critical step in organelle isolation, as its composition governs both the efficiency of homogenization and the integrity of the recovered structures. Buffer components must be carefully optimized to preserve organelle stability while enabling effective cell disruption. An unsuitable formulation can compromise purification by promoting organelle damage or contamination, whereas a well-designed buffer ensures compatibility with downstream analytical techniques.[15]

Once organelles are released, they can be enriched by a range of separation techniques (Table 1).

Differential centrifugation separates organelles based on their size and sedimentation coefficient through the application of gradual increases in centrifugal force. Larger and denser structures, such as nuclei and mitochondria, sediment at lower speeds, whereas smaller vesicles require higher centrifugal forces. This approach is simple, rapid, and widely accessible, making it a common first-step enrichment strategy. However, it provides limited purity and is prone to cross-contamination, due to co-sedimentation of organelles with similar size and density, leading to composite signals and potential metabolite leakage during processing.[42,43]

In contrast, density-gradient centrifugation exploits differences in buoyant density. The homogenate is layered onto a continuous or discontinuous gradient, usually made of sucrose, Percoll or iodixanol, and centrifuged until each organelle reaches its isopycnic point. This results in the formation of distinct bands, allowing improved resolution between mitochondria, lysosomes, peroxisomes and endoplasmic reticulum fragments. Compared to differential centrifugation, it provides higher resolution and improved enrichment of major organelles. Nevertheless, the technique is more time-consuming and can induce osmotic stress from the gradient media, promoting leakage of polar metabolites, redistribution along the gradient, and ion suppression in downstream MS analysis.[42,43]

The optimization of a fractionation workflow requires careful consideration of the available biological material and the sensitivity of the analytical techniques employed. These parameters play a central role in experimental design, as they directly influence the reliability and interpretability of the results. This is particularly relevant in metabolomics and lipidomics, where analyte levels are highly dynamic and susceptible to rapid fluctuations, necessitating stringent control of experimental conditions.[44]

Free-flow electrophoresis offers a complementary separation strategy by exploiting differences in surface charge and electrophoretic mobility. Organelles are separated within a laminar buffer flow under an applied electric field, making this technique relatively gentle and better suited for preserving membrane integrity compared to centrifugation-based methods. However, it has low throughput, requires specialized equipment, and separation is based on surface charge, which may not reflect true organelle identity and can introduce bias toward more stable or highly charged membrane structures.[42,45]

Differential filtration uses membranes with precisely defined pore sizes to mechanically separate organelles according to their physical diameter. This method is rapid and does not require density media. However, resolution is limited, membranes are prone to clogging, and mechanical shear can rupture fragile organelles, leading to loss of small or deformable organelles and release of soluble metabolites.[45,46]

Affinity purification utilizes highly specific antibody–antigen or ligand–receptor interactions. Organelles expressing specific surface markers are captured on magnetic supports or columns, enabling selective isolation. This approach offers high specificity when suitable markers are available. However, it depends on antibody quality, can suffer from non-specific binding, and inherently isolates only marker-positive subpopulations, introducing representation bias and potentially altering organelle surface composition.[45,46]

Fluorescence-activated organelle sorting (FAOS) extends principles similar to fluorescence-activated cell sorting to subcellular level. Organelles are labeled with specific fluorescent dyes or genetically encoded fluorescent proteins and subsequently high-speed sorted. This approach enables high-purity isolation and can reach single-organelle resolution. However, it requires prior labeling, involves instrument complexity and potential phototoxicity, and only tagged organelles are recovered, introducing labeling bias and potential perturbation of native composition.[47]

Magnetic nanoparticle-based isolation relies on magnetic nanoparticles conjugated to organelle-specific antibodies. After incubation, the labeled organelles are rapidly separated by applying an external magnetic field. This method is rapid, scalable, and compatible with downstream MS workflows. However, it requires accessible surface markers, can cause

Table 1 Overview of subcellular fractionation methods, highlighting their main advantages and associated analytical artefacts

Subcellular fractionation methods

Method	Advantages	Disadvantages/analytical artefacts
Differential centrifugation [42,43] 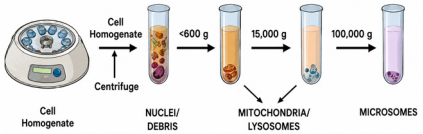	- Simple and rapid - Widely accessible - Scalable	- Low purity and high cross-contamination - Co-sedimentation of organelles with similar size/density - Artificial mixing of compartments leading to composite signals - Metabolite leakage during prolonged processing
Density-gradient centrifugation [42,43] 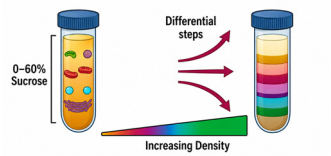	- Improved resolution between major organelles - Better enrichment than differential centrifugation	- Time-consuming - Osmotic stress from gradient media - Leakage of polar metabolites across membranes - Redistribution of small molecules along the gradient
Free-flow electrophoresis [42,45] 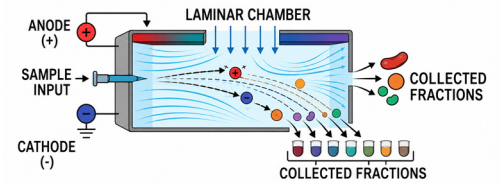	- Gentle separation - Preserves membrane integrity better than centrifugation	- Low throughput - Requires specialized equipment - Separation based on surface charge may not reflect true biological identity - Bias toward stable membrane-bound structures
Differential filtration [45,46] 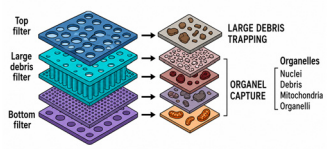	- Fast and simple - No density media required	- Limited resolution - Risk of clogging - Mechanical stress causing membrane rupture - Loss of small or deformable organelles
Affinity purification [45,46] 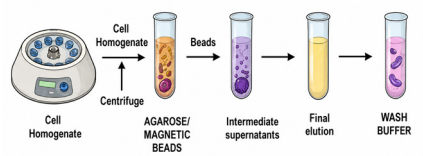	- High specificity for target organelles - Selective enrichment	- Dependent on antibody quality - Non-specific binding - Selective isolation of subpopulations (biased representation) - Potential alteration of organelle surface and composition
Fluorescence-activated organelle sorting (FAOS) [47] 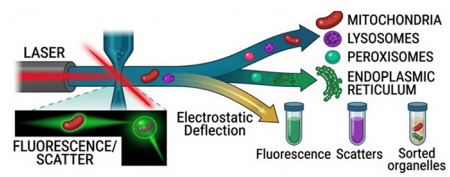	- High purity - Ability to isolate subpopulations - Single-organelle level resolution	- Requires labeling - Phototoxicity and instrument complexity - Label-dependent bias (only tagged organelles detected) - Alteration of native composition due to fluorescent tagging
Magnetic nanoparticle isolation [45,48] 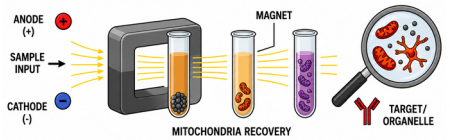	- Very fast - Scalable - Compatible with downstream MS	- Requires surface markers - Possible membrane damage - Non-uniform labeling efficiency - Physical perturbation of membranes and associated metabolites/lipids
Chromatographic solid-phase separation [45,49] 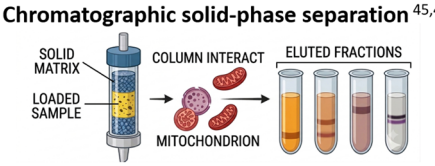	- Combines multiple separation principles - Potential for fine resolution	- Risk of non-specific adsorption - Variable recovery - Loss of metabolites due to interaction with stationary phase - Distortion of quantitative profiles through differential retention

membrane damage, and variable labeling efficiency may lead to incomplete or uneven recovery, affecting quantitative reliability.[45,48]

Finally, chromatographic solid-phase separation sorts organelles based on their differential interaction with stationary phase, as in size-exclusion, ion-exchange or hydrophobic interaction chromatography. By combining multiple separation principles, it can achieve high resolution under optimized conditions. However, there is a risk of non-specific adsorption, variable recovery, and distortion of quantitative profiles due to differential retention and interaction with the stationary phase.[45,49]

As summarized in Table 1, fractionation-based approaches remain widely used despite their well-known methodological limitations. These workflows inherently introduce analytical artefacts, including metabolite leakage, lipid exchange, residual enzymatic activity, and ion suppression from buffer components. These effects complicate quantitative interpretation and highlight the need for rigorous controls, including organelle marker proteins, internal standards, and complementary validation strategies such as imaging-based approaches.[45]

A critical step in fractionation workflows is the characterization of the obtained fractions. Because most isolation strategies yield enriched rather than pure organelle populations, validation of enrichment and cross-contamination is essential. This is typically addressed through orthogonal approaches such as Western Blot (WB), enzymatic assays, or targeted proteomics on organelle marker proteins.[50,51] While these approaches have limitations, they provide a widely accepted framework for assessing fraction quality. Integration with quantitative proteomics and imaging further improves evaluation of fraction integrity.[52,53] In this context, subcellular MS data should be interpreted as relative enrichments within characterized fractions rather than absolute compartment-specific concentrations.

While fractionation enables physical access to subcellular compartments, it also introduces multiple sources of analytical bias. These limitations become particularly evident during downstream MS analysis of the isolated fractions, as discussed below.

3.2 Analysis of subcellular fractions by MS-based metabolomics and lipidomics

Once the enriched organelle fractions are obtained, analysis typically proceeds through solvent extraction followed by mass spectrometry analysis. Polar metabolites are typically extracted using cold solvent systems (*e.g.*, methanol/water mixtures), often combined with chemical derivatization. Dansyl labeling is widely used to enhance sensitivity and coverage in LC-MS/MS workflows,[44] while for primary metabolites such as organic acids, amino acids and sugars, gas chromatography-mass spectrometry (GC-MS) following methoximation and trimethylsilylation (TMS) derivatization remains a powerful complementary strategy.[54,55]

Conversely, lipid fractions are typically extracted using liquid–liquid protocols based on *tert*-butyl ether (MTBE)/methanol/water solutions. This approach efficiently separates the lipid phase and reduces interference from salts and buffer components.[56] Lipid extracts are subsequently analyzed by reversed-phase LC-MS (RP-LC-MS) for detailed acyl-chain profiling, and/or by shotgun lipidomics (direct infusion) when sample availability is limited. Importantly, lipids benefit from greater stability due to membrane anchoring and slower turnover, more robust compartmental profiles compared to polar metabolites.[42,57]

3.3 Spatial metabolomics: *in situ* imaging

To maintain native spatial organization and avoid the artefacts associated with organelle isolation, such as metabolite leakage, residual enzymatic activity, and redistribution of molecules, *in situ* mass spectrometry imaging techniques represent particularly attractive analytical strategies (Fig. 3).

Among these, Secondary Ion Mass Spectrometry (SIMS), and in particular nanoscale SIMS (NanoSIMS), provides the highest spatial resolution currently achievable in MS-based imaging. NanoSIMS employs a focused primary ion beam to sputter the sample surface, generating secondary ions that are subsequently analyzed. This enables high-resolution spatial mapping of elemental and isotopic distributions at the subcellular level. The lateral resolution can reach ~50–100 nm, enabling sub-organelle analysis and direct visualization of isotope incorporation into target lipid classes and metabolites in stable isotope tracing experiments.[58,59] In recent years, several studies have successfully applied NanoSIMS to image intracellular lipid trafficking, membrane dynamics, and metabolite incorporation at subcellular resolution, demonstrating its utility for spatially resolved metabolic investigations.[58,60,61]

Because NanoSIMS primarily detects secondary ions generated from the sample surface, intracellular organelles generally need to be exposed prior to analysis, either through ultramicrotome sectioning of the cell or by sequential sputtering/depth-profiling approaches when intact cells are analysed.[58]However, as NanoSIMS is primarily an elemental and isotopic imaging technique, its ability to unambiguously identify intact molecular species is inherently limited compared with LC-MS-based approaches. Moreover, absolute quantification remains challenging due to matrix-dependent ion yields and the requirement for appropriate calibration standards. As a result, NanoSIMS is most effectively applied to probe metabolic activity through isotopic enrichment rather than to provide comprehensive molecular profiling (Fig. 3a). Beyond conventional NanoSIMS workflows, recent SIMS-based platforms such as 3D OrbiSIMS have demonstrated label-free metabolic imaging with subcellular lateral resolution and improved mass-resolving power, further expanding the analytical potential of spatially resolved intracellular metabolomics.[62]

In contrast, Matrix-Assisted Laser Desorption/Ionization Mass Spectrometry Imaging (MALDI-MSI)[63–65] and Desorption Electrospray Ionization Mass Spectrometry Imaging

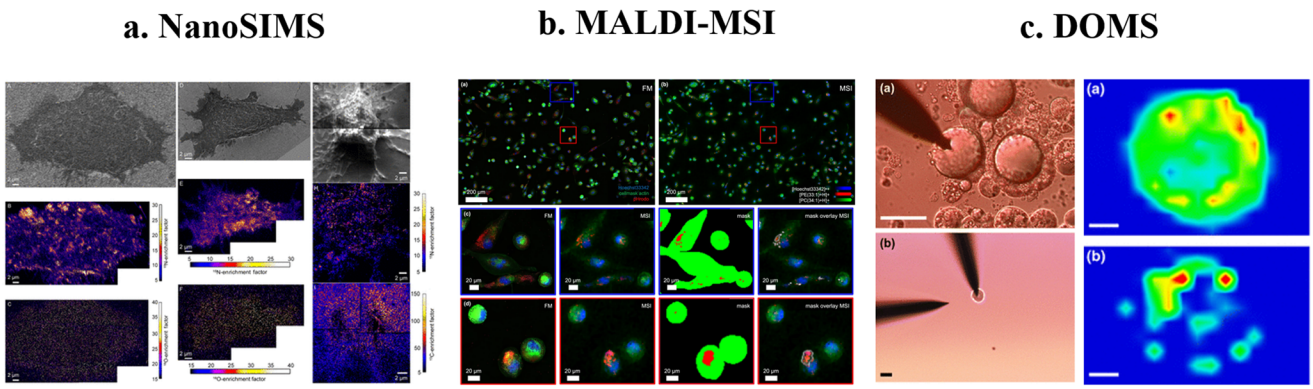

Fig. 3 Representative examples of subcellular molecular imaging by mass spectrometry-based techniques. (a) NanoSIMS imaging of cholesterol and sphingolipid distributions at nanometer spatial resolution, enabling visualization of subcellular lipid heterogeneity *via* isotopic labelling. (b) Single-cell MALDI-MSI integrated with optical microscopy, allowing spatially resolved molecular profiling correlated with cellular morphology. (c) DOMS coupled with nanomanipulation, enabling isolation and chemical analysis of individual organelles and revealing intra-cellular compositional variability. Images reproduced/adapted from ref. 58 for NanoSIMS, from ref. 67 for MALDI-MSI, and from ref. 71 for DOMS.

(DESI-MSI)[66] provide broader molecular coverage, enabling the detection of hundreds of metabolites and lipids in a single experiment. In MALDI-MSI, analytes are co-crystallized with an organic matrix that facilitates laser-induced desorption and ionization, allowing high sensitivity and broad molecular coverage, particularly for lipid species. DESI-MSI, in contrast, operates under ambient conditions by directing a charged solvent spray onto the sample surface, enabling ionization with minimal sample preparation, albeit generally with lower spatial resolution and sensitivity compared to MALDI. These techniques generally lack the subcellular resolution necessary to distinguish individual organelles, as their lateral resolution typically ranges from 5 to 50 μm. Consequently, while MALDI- and DESI-MSI are powerful tools for tissue-level and cellular spatial metabolomics and lipidomics, their ability to resolve true organelle-specific distributions remains limited. However, recent advances in transmission-mode geometry and laser post-ionization strategies have started to push MALDI-MSI towards true subcellular resolution, achieving pixel sizes approaching 1 μm while preserving broad molecular coverage for lipids and metabolites[67] (Fig. 3b).

A complementary strategy linking physical isolation and direct MS analysis is Direct Organelle Mass Spectrometry (DOMS). In this approach, individual organelles are selectively micro-aspirated under microscopic visualization and directly analyzed by nanospray MS, bypassing the redistribution artefacts associated with bulk isolation.[68–70] This strategy preserves molecular information at the level of isolated organelles and has been primarily applied to the analysis of lipid composition, particularly in lipid droplets. However, DOMS remains technically demanding and low-throughput, and its application to comprehensive metabolomics is still limited. In addition, potential contamination during micro-manipulation and the very small sample amounts complicate quantitative analysis (Fig. 3c).

Taken together, these workflows highlight that method-induced distortion is analyte-specific: membrane-anchored lipids generally exhibit greater stability than soluble, fast-turnover metabolites. More broadly, they illustrate a central analytical trade-off in spatial metabolomics: techniques providing the highest spatial resolution (*e.g.*, NanoSIMS) offer limited molecular specificity, whereas approaches enabling broad molecular coverage (*e.g.*, MALDI- and DESI-MSI) operate at lower spatial resolution.

3.4 Representative applications and methodological trade-offs

Recent applications in subcellular metabolomics and lipidomics have highlighted both the transformative analytical potential of organelle-resolved workflows and the methodological compromises that still limit their widespread implementation. Importantly, the robustness of subcellular measurements strongly depends not only on the analytical platform employed, but also on the structural and biochemical properties of the investigated organelles.

Mitochondria currently represent one of the most analytically accessible targets for subcellular metabolomics. Their relatively large size, double-membrane architecture, and established purification workflows enable comparatively robust enrichment with limited cross-contamination. Recent studies combining rapid immunocapture approaches with LC-MS analysis successfully characterized compartment-specific TCA intermediates, acyl-carnitines, and redox metabolites while partially minimizing post-isolation metabolic drift.[21,41] These studies demonstrated how organelle-resolved metabolomics can uncover localized metabolic regulation that remains obscured in bulk-cell analyses. Importantly, the main analytical advantage of these workflows is not absolute purity, but speed: by shortening the interval between quenching and extraction, rapid immunocapture better preserves relative mitochondrial enrichment patterns than conventional centrifugation-based protocols. At the same time, these studies also indicate that the most reliable compartment-specific readouts are obtained for metabolites that are sufficiently abun-

dant and less prone to rapid exchange, whereas adenylates and other highly diffusible species remain particularly vulnerable to distortion. Nevertheless, even mitochondrial workflows remain highly sensitive to incomplete metabolic quenching and leakage of highly diffusible metabolites such as ATP, NAD(H), and glycolytic intermediates.

In contrast, lysosomal metabolomics remains substantially more challenging. Lysosomes are highly dynamic and fragile organelles characterized by acidic luminal pH and elevated hydrolytic activity, making them particularly susceptible to metabolite redistribution during isolation. Affinity purification strategies such as LysoIP workflows enabled the characterization of lysosome-specific metabolite pools and nutrient sensing pathways.[34] However, these studies also highlighted the difficulty of preserving native metabolite concentrations during fractionation, especially for small polar compounds that rapidly diffuse across partially compromised membranes. Consequently, lysosomal metabolomics currently remains more vulnerable to preparation-induced artefacts compared with mitochondrial enrichment workflows, further emphasizing how analytical distortions in subcellular omics are highly organelle- and analyte-dependent. Thus, LysoIP-based workflows are especially powerful for identifying qualitative pathway relationships and nutrient-sensing signatures, but are less secure when used to infer absolute lysosomal concentrations of small polar metabolites. This contrast with mitochondrial workflows illustrates a broader analytical principle: the success of subcellular metabolomics depends not only on instrumental sensitivity, but also on the intrinsic physical stability of the target organelle during isolation.

Beyond organelle-specific isolation challenges, spatially resolved and single-organelle mass spectrometry approaches have recently enabled direct investigation of intracellular metabolic heterogeneity while partially minimizing redistribution artefacts associated with bulk fractionation workflows.

The NanoSIMS example shown in Fig. 3a illustrates isotopic enrichment localized within intracellular membrane-rich regions following stable isotope tracing experiments. In the studies summarized by Brunet and Kraft, mammalian cells and tissue models were supplemented with isotopically labelled metabolic precursors, such as ^{13}C- or ^{15}N-labelled lipids, in order to track intracellular lipid incorporation and membrane remodeling processes at nanometer-scale lateral resolution.[58] The resulting NanoSIMS images enabled visualization of localized isotope accumulation within distinct subcellular regions, revealing heterogeneous lipid turnover and intracellular trafficking patterns that would remain inaccessible in bulk analyses. In particular, the image reported in Fig. 3a highlights the capability of NanoSIMS to spatially resolve metabolically active membrane domains and intracellular lipid incorporation with exceptional spatial precision. At the same time, these studies also emphasized important analytical limitations associated with NanoSIMS workflows, including relatively limited molecular specificity, demanding sample preparation requirements, and the need for sectioning or depth-profiling strategies to expose intracellular structures prior to analysis. In this context, the analytical strength of NanoSIMS lies less in comprehensive molecular annotation than in its ability to localize isotopically labelled metabolic activity with unmatched spatial precision. NanoSIMS is therefore best viewed as a hypothesis-testing and validation tool for intracellular flux and membrane remodelling, rather than as a stand-alone platform for broad metabolite identification.

The MALDI-MSI example shown in Fig. 3b highlighted recent progress toward near-subcellular lipid imaging in intact biological samples. In particular, Potthoff *et al.* combined transmission-mode MALDI-MSI with integrated optical microscopy and advanced ion optics to investigate intracellular lipid heterogeneity in single mammalian cells undergoing phagocytosis as well as in tumor-infiltrating neutrophils within tissue sections.[64,65,67] Their workflow enabled visualization of chemically distinct intracellular regions and revealed heterogeneous lipid distributions associated with different cellular states and microenvironments while preserving broad molecular coverage at micrometer-scale spatial resolution. Importantly, the study demonstrated how multimodal integration between microscopy and MSI can substantially improve the interpretation of intracellular chemical heterogeneity by correlating molecular information with cellular morphology and spatial organization. Nevertheless, accurate assignment to specific organelles remains challenging because of residual spatial overlap, ion suppression effects, and limited three-dimensional resolution in densely packed intracellular environments.

Additional subcellular MSI and SIMS studies further support this trend, showing that improvements in ion optics and high-resolution imaging platforms can reveal intracellular chemical heterogeneity beyond conventional tissue-scale MSI, but do not fully eliminate the trade-off between localization accuracy, confident molecular assignment, and quantitative robustness. Accordingly, these approaches are particularly informative when interpreted together with orthogonal workflows such as organelle enrichment, targeted MS, or stable isotope tracing.

Finally, the DOMS workflow (Fig. 3c) demonstrated direct aspiration and nanospray ionization of individual lipid droplets from differentiated 3T3-L1 murine adipocytes, enabling characterization of single-organelle triacylglycerol (TAG) composition with minimal sample processing.[71] Using nanomanipulation-coupled MALDI-DOMS, the study revealed substantial lipid heterogeneity between individual lipid droplets that would otherwise be masked in bulk-cell lipidomics experiments. The work also demonstrated improved ionization efficiency, longer acquisition times, and MS/MS capabilities compared with previous NSI-DOMS approaches. However, the study simultaneously emphasized several practical limitations of single-organelle workflows, including low throughput, extremely limited sample amounts, and the difficulty of achieving robust quantitative standardization during micromanipulation. In this sense, DOMS occupies a distinct analytical niche: it sacrifices throughput and standardization in exchange for maximal proximity to the native chemical content of individual organelles.

Collectively, these representative applications demonstrate that no current methodology simultaneously achieves high spatial resolution, broad molecular coverage, quantitative robustness, and high throughput. Instead, each workflow involves distinct trade-offs between localization accuracy, analytical depth, sample integrity, and experimental scalability.

4. Metabolomics *versus* lipidomics at the organelle level

Recent subcellular studies highlight a critical analytical aspect: lipidomics behaves far more robustly than metabolomics during organelle purification.[72] This distinction depends primarily on fundamental differences in molecular turnover and physical properties. As the structural scaffold of organelles, lipids are integrated into membranes, and their hydrophobic nature and strong membrane association allow them to resist redistribution during subcellular fractionation.[16] Furthermore, the slow turnover rates of most structural lipids, ranging from minutes to hours, allow them to remain stable during the isolation window without significant degradation.[73,74]

In contrast, the subcellular metabolome is characterized by high dynamic variability. Small polar metabolites, such as TCA cycle intermediates or nucleotides, exhibit very high turnover rates (milliseconds to seconds), making them highly susceptible to post-collection enzymatic activity and metabolic shifting if quenching is not instantaneous.[15,24] Moreover, their high aqueous solubility leads to leakage across compromised organelle membranes, often resulting in underestimation of true compartmental concentrations.[75,76]

From an MS perspective, lipidomics also benefits from cleaner extraction protocols (*e.g.* liquid–liquid extraction) which effectively remove salts and osmotic agents that would otherwise cause severe ion suppression in polar metabolomics workflows.[77] As a result, lipid measurements are generally less affected by matrix effects and signal distortion. Consequently, while organelle-resolved metabolomics often yields a partial and potentially biased representation of the most abundant species, lipidomics provides a more accurate reflection of compartmental specificity, maintaining high spatial and molecular resolution.[78]

These analytical differences directly impact data interpretation and the reliability of biological conclusions.

5. Data interpretation and analytical limits

5.1 Data interpretation and quantitative limitations

A central challenge in organelle-resolved MS analysis is distinguishing accurate subcellular localization from technical artifacts introduced during isolation and extraction. The detection of a metabolite or lipid within a purified fraction does not necessarily reflect its functional compartmentalization, especially for highly mobile polar metabolites.[15,40] Quantitative interpretation is further complicated by limited sample amounts, variable recovery, and matrix effects, and the fact that virtually all fractionation methods produce enriched fraction rather than pure organelles.

5.2 Key analytical challenges and artefacts

Several recurring artifacts can compromise the reliability of subcellular metabolomics and lipidomics data (Table 2).

Incomplete quenching represents a major concern for labile metabolites such as nucleotides, redox cofactors (NAD^+/NADH, $NADP^+$/NADPH) and glycolytic intermediates. Their rapid turnover allows residual enzymatic activity that could alter metabolite pools before the extraction procedure.[79]

Similarly, leakage and unintended mixing occur when organelle membranes integrity is compromised during homogenization or centrifugation steps, leading to the redistribution of soluble compounds into non-native compartments and causing underestimation of true compartment-specific concentrations.[15,80]

Cross-contamination further complicates analysis. In fact, co-sedimentation or incomplete separation of organelles with similar physicochemical properties generates mixed profiles that cannot be unambiguously assigned to a single compartment.[45]

Moreover, differential extraction bias originates from the unequal solubility of metabolites in isolation buffers and extraction solvents, often resulting in selective loss or over-recovery of certain compound classes.[44]

Ion suppression, typically induced by salts, sucrose, Percoll or other gradient media carried over from density gradients, strongly suppress ionization, particularly affecting low-abundance polar analytes in LC-MS workflows.[44,81]

As previously discussed, lipidomics is generally more robust against these issues because structural lipids are physically anchored at membranes and exhibit slower turnover rates, whereas small polar metabolites are highly diffusible and with very fast turnover (milliseconds to seconds).[82,83]

5.3 Organelle purity, validation and normalization

Virtually no subcellular isolation method yields absolute purity. Residual material from adjacent compartments or membrane fragments is almost inevitable, even under optimized conditions.[15,45] Consequently, subcellular MS profiles should be interpreted as relative enrichments within well-characterized fraction rather than absolute compartment-specific concentrations. Fraction quality is typically assessed by western blotting, enzymatic assay or quantitative proteomics using multiple organelle makers.[84–86] Protein correlation profiling and complementary imaging further improve confidence in the enrichment levels. Even with these controls, minor contaminants may remain undetected, making orthogonal validation (*e.g.*, NanoSIMS or DOMS), highly advisable when possible.[69,87]

Accurate comparisons between organelles or conditions requires careful normalization. Total protein content remains

Table 2 Common analytical artefacts in subcellular metabolomics and lipidomics, their impact on measurements, and mitigation strategies

Analytical artefacts		
Artefact	Impact on measurements	Mitigation strategies
Incomplete quenching [79] 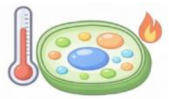	Residual enzymatic activity after sampling induces rapid alterations in labile metabolites (*e.g.*, nucleotides, redox cofactors, glycolytic intermediates), distorting the native metabolic state	- Rapid quenching protocols combining snap-freezing with cold, acidified solvents - Minimization of processing time - Implementation of microfluidic or fast-sampling approaches
Metabolite leakage [15,80] 	Loss and redistribution of soluble metabolites due to compromised organelle membranes, leading to underestimation of compartment-specific concentrations	- Gentle cell disruption - Rapid processing - Use of isotonic and stabilizing buffers - Validation of compartment integrity using imaging or marker assays
Cross-contamination [45,90] 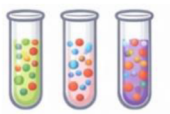	Co-isolation of organelles with similar physicochemical properties generates mixed fractions that do not represent a single compartment	- Rigorous fraction characterization (*e.g.*, western blot, enzymatic assays, quantitative proteomics with multiple markers) - Protein correlation profiling - Orthogonal validation strategies
Differential extraction bias [44] 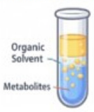	Unequal extraction efficiencies due to differences in metabolite solubility across isolation and extraction solvents, resulting in selective loss or under-recovery of specific metabolite classes	- Optimization of extraction protocols for each fraction - Use of class-specific internal standards - Evaluation and reporting of extraction recoveries
Ion suppression [44,81] 	Carry-over of salts and buffer components (*e.g.*, sucrose, mannitol) reduces ionization efficiency in MS, particularly affecting low-abundance polar metabolites	- Removal of interfering components through sample clean-up (*e.g.*, liquid–liquid extraction, desalting) - Use of matrix-matched calibration - Optimization of LC-MS conditions

the most practical and widely used approach, since it assumes relatively constant protein-to-volume ratios across different compartments.

This assumption may not be universally valid, particularly when comparing organelles with very different membrane densities or metabolic roles.[21] Alternative strategies based on estimated organelle volume or total cell/organelle number may provide a closer link to absolute quantities, but they are technically more demanding and prone to propagate measurement errors. The most transparent practice is to report results obtained with multiple normalization methods and clearly state which was used for each presented dataset.[88]

5.4 Implications and mitigation strategies

Apparent compartmental shifts observed in subcellular datasets may in reality reflect technical artefacts (incomplete quenching, leakage, cross-contamination, matrix effect) rather than biological changes.

Conversely, real localized metabolic changes may be masked or underestimated due to low fraction purity and inappropriate normalization.[15,80] In pathological contexts, this risk is particularly high where metabolic variation in different organelles may be covered at the bulk level or produce misleading enrichment profiles.

To maximize reliability and mitigate these challenges several useful strategies could be implemented. Rapid quenching protocols, combining snap-freezing with acidified cold solvents or integrated microfluidic approaches, should be preferred whenever possible.[79,89] Fraction purity should be assessed using multiple orthogonal markers and, when feasible, protein correlation validation.[90,91] Furthermore, normalization should never rely on a single proxy; reporting results obtained with different strategies (protein content, estimated organelle volume, and cell/organelle number) greatly improves transparency.[88] In addition, the use of complementary spatial MS techniques such as NanoSIMS or direct organelle nanospray-MS can provide independent confirmation of metabolite distributions, thereby reducing over-reliance on classical fractionation methods.[90]

By systematically applying these mitigation strategies and maintaining transparent reporting of experimental limitations, researchers can substantially increase the reliability and biological relevance of subcellular metabolomics and lipidomics studies.

6. Future perspective and concluding remarks

The field of organelle-resolved metabolomics and lipidomics is advancing rapidly, driven by the growing awareness that subcellular compartmentalization must be treated as a key analytical variable rather than a secondary biological feature. While current methods have already exposed important limitations, they have also opened several promising directions to improve both data quality and interpretation.

6.1 Integrating organelle-resolved metabolomics with isotope tracing

Combining subcellular fractionation or spatial MS with stable isotope tracing represents one of the most powerful approaches. Unlike steady-state measurements, isotope labeling enables the measurement of compartment-specific metabolic fluxes.[92–94] For example, tracing substrates such as ^{13}C-glucose or ^{15}N-glutamine in mitochondria- or in lysosomes-enriched fractions can uncover localized pathway activity hidden in bulk analyses.[34,93]

However, this approach introduces technical challenges, including partial loss of isotopic enrichment during long isolation procedures and temporal mismatches between labeling dynamics and organelle separation.[92,95] In addition, the resulting isotopologue patterns are often complex and difficult to interpret without dedicated modelling frameworks. Future progress will likely depend on faster isolation workflows (*e.g.*, microfluidic platforms), and improved computational models capable of resolving complex isotopologue patterns in subcellular datasets.[96,97]

6.2 Multi-omics integration on the same fraction

Performing metabolomics, lipidomics and proteomics on the same subcellular fraction offers significant advantages by reducing inter-sample variability and enabling direct correlation between metabolite/lipids and the enzymes or transporter of that compartment. In particular, protein correlation profiling has emerged as a valuable tool to assess organelle enrichment while simultaneously linking metabolic changes to the presence of specific enzymes or transport systems.[98–100] This type of workflow reduces inter-sample variability and enables a more direct interpretation of proteome–metabolome relationships within defined compartments.

Realizing the full potential of this strategy requires robust protocols for parallel extraction of the different molecular classes from the same, limited material, as well as unified bioinformatics pipelines that can integrate multi-omics.[101,102]

6.3 Emerging single-cell and single-organelle technologies

Significant advances are expected from single-cell and single-organelle approaches. Techniques such as fluorescence-activated organelle sorting (FAOS), DOMS, and improved high-resolution imaging (NanoSIMS and next-generation MALDI-MSI).[103–106]

Although these methods currently face limitations in sensitivity and throughput their combination with multiplexed isotope tracing or with live-cell imaging, hold great promise for studying dynamic, compartment-specific metabolism at subcellular resolution.[104,107]

6.4 The role of artificial intelligence and machine learning

Artificial intelligence and machine learning are increasingly applied to subcellular datasets for tasks such as deconvoluting composite signals from mixed fractions, predicting subcellular localization from bulk omics data, and optimizing normalization strategies.[108–110]

When carefully validated against experimental ground-truth data (*e.g.*, imaging or isotope tracing) these tools can help mitigate some inherent analytical limitations. However, without rigorous validation there is a real risk that may reinforce rather than resolve underlying artefacts.[109,111]

6.5 Concluding remarks

Organelle-resolved metabolomics and lipidomics have highlighted fundamental analytical constraints that are inherent to mass spectrometry-based measurements in spatially organized eukaryotic cells. By explicitly considering compartmentalization as an analytical variable, and systematically addressing issues of quenching, purity, extraction bias, and quantification, the field can move beyond averaged bulk signal toward a more accurate, spatially resolved understanding of cellular metabolism. The most impactful advances will arise from combining complementary approaches, including fractionation with spatial imaging, isotope tracing, multi-omics integration, and data-driven computational methods, while maintaining transparent reporting of methodological limitations.[94,102,107,110]

This integrated approach will be essential for uncovering compartment-specific mechanisms in complex disease, such as cancer and neurodegeneration, and supporting more precise mechanistically informed therapeutic strategies.[34,106,111]

Author contributions

M. N.: conceptualization, investigation, writing – original draft, data curation, visualization. S. S.: writing – original draft, investigation, data curation, visualization. E. B.: writing – review & editing. F. Re: writing – review & editing. F. Raimondo: writing – review & editing, validation. G. P.: conceptualization, writing – review & editing, supervision.

Conflicts of interest

Giuseppe Paglia reports employment with the University of Milan-Bicocca, Department of Medicine and Surgery. All other authors declare no competing financial interests or personal relationships that could have appeared to influence the work reported in this paper.

Abbreviations

ABC	ATP-binding cassette (transporters)
AI	Artificial intelligence
ATP	Adenosine triphosphate
DBS	Dried blood spots
DESI-MSI	Desorption electrospray ionization mass spectrometry imaging
ER	Endoplasmic reticulum
FAOS	Fluorescence-activated organelle sorting
FFA	Free fatty acid
GC-MS	Gas chromatography-mass spectrometry
HMDB	Human Metabolome Database
LC-MS	Liquid chromatography-mass spectrometry
MALDI-MSI	Matrix-assisted laser desorption/ionization mass spectrometry imaging
MS	Mass spectrometry
MTBE	Methyl *tert*-butyl ether
NAD^+/NADH	Nicotinamide adenine dinucleotide (oxidized/reduced)
$NADP^+$/NADPH	Nicotinamide adenine dinucleotide phosphate (oxidized/reduced)
NanoSIMS	Nanoscale secondary ion mass spectrometry
ROS	Reactive oxygen species
RP-LC-MS	Reversed-phase liquid chromatography-mass spectrometry
SIMS	Secondary ion mass spectrometry
SLC	Solute carrier (transporters)
TCA	Tricarboxylic acid (cycle)
TMS	Trimethylsilylation

Data availability

Data availability is not applicable as no new data were generated or analyzed in this review.

Supplementary information (SI): supplementary Tables S1 and S2 are provided as an Excel file containing multiple worksheets. A description of each worksheet is included in a dedicated README sheet. See DOI: https://doi.org/10.1039/d6an00535g.

Acknowledgements

The authors thank colleagues and collaborators for helpful discussions.

References

1 S. J. T. Guttorm, S. R. H. Wilson, E. K. Amundsen, H. Rootwelt and K. B. P. Elgstøen, *Anal. Chim. Acta*, 2025, **1371**, 344426.
2 E. Bossi, E. Limo, L. Pagani, N. Monza, S. Serrao, V. Denti, G. Astarita and G. Paglia, *Metabolites*, 2024, **14**, 46.
3 E. Bossi, M. Nobile, F. Paoletti, L. Ticini, S. Serrao, A. Giglio, G. Parati, A. Zaza, L. Crotti, G. Malfatto and G. Paglia, *J. Proteome Res.*, 2026, **25**, 1636–1646.
4 S. Serrao, E. Bossi, V. Denti, J. Burtscher, M. Faulhaber, G. Weiss, W. Schobersberger, T. Dünnwald and G. Paglia, *Biochim. Biophys. Acta, Mol. Cell Biol. Lipids*, 2025, **1870**, 159647.
5 S. Dolci, L. Mannino, E. Bottani, A. Campanelli, M. Di Chio, S. Zorzin, G. D'Arrigo, A. Amenta, A. Segala, G. Paglia, V. Denti, G. Fumagalli, E. Nisoli, A. Valerio, C. Verderio, G. Martano, F. Bifari and I. Decimo, *Pharmacol. Res.*, 2022, **178**, 106149.
6 C. Volani, G. Paglia, S. V. Smarason, P. P. Pramstaller, E. Demetz, C. Pfeifhofer-Obermair and G. Weiss, *Cells*, 2018, **7**, 264.
7 S. Yang and Y. Wu, *Front. Cardiovasc. Med.*, 2025, **12**, 1656113.
8 A. Leiherer, A. Muendlein, C. H. Saely, R. Laaksonen, P. Fraunberger and H. Drexel, *Eur. Heart J. Open*, 2024, **4**, DOI: 10.1093/ehjopen/oeae001.
9 T. J. Wang, M. G. Larson, R. S. Vasan, S. Cheng, E. P. Rhee, E. McCabe, G. D. Lewis, C. S. Fox, P. F. Jacques, C. Fernandez, C. J. O'Donnell, S. A. Carr, V. K. Mootha, J. C. Florez, A. Souza, O. Melander, C. B. Clish and R. E. Gerszten, *Nat. Med.*, 2011, **17**, 448–453.
10 C. J. Lynch and S. H. Adams, *Nat. Rev. Endocrinol.*, 2014, **10**, 723–736.
11 L. M. Butler, Y. Perone, J. Dehairs, L. E. Lupien, V. de Laat, A. Talebi, M. Loda, W. B. Kinlaw and J. V. Swinnen, *Adv. Drug Delivery Rev.*, 2020, **159**, 245–293.
12 F. Perrotti, C. Rosa, I. Cicalini, P. Sacchetta, P. Del Boccio, D. Genovesi and D. Pieragostino, *Int. J. Mol. Sci.*, 2016, **17**, 1992.
13 A. Esposito, T. Seri, M. Breccia, M. Indrigo, G. De Rocco, F. Nuzzolillo, V. Denti, F. Pappacena, G. Tartaglione, S. Serrao, G. Paglia, L. Murru, S. de Pretis, J.-M. Cioni, N. Landsberger, F. C. Guarnieri and M. Palmieri, *EMBO Mol. Med.*, 2024, **16**, 2795–2826.
14 J. Matuszczyk, A. Teleki, J. Pfizenmaier and R. Takors, *Biotechnol. J.*, 2015, **10**, 1639–1650.
15 S. Qin, Y. Zhang, Y. Tian, F. Xu and P. Zhang, *J. Pharm. Biomed. Anal.*, 2022, **210**, 114557.
16 T. Harayama and H. Riezman, *Nat. Rev. Mol. Cell Biol.*, 2018, **19**, 281–296.
17 A. Ballabio and J. S. Bonifacino, *Nat. Rev. Mol. Cell Biol.*, 2020, **21**, 101–118.
18 C. Zampieri, C. Ganini and G. Melino, *Cell Death Dis.*, 2020, **11**, 259.
19 D. S. Wishart, A. Guo, E. Oler, F. Wang, A. Anjum, H. Peters, R. Dizon, Z. Sayeeda, S. Tian, B. L. Lee, M. Berjanskii, R. Mah, M. Yamamoto, J. Jovel, C. Torres-Calzada, M. Hiebert-Giesbrecht, V. W. Lui, D. Varshavi, D. Varshavi, D. Allen, D. Arndt, N. Khetarpal, A. Sivakumaran, K. Harford, S. Sanford, K. Yee, X. Cao, Z. Budinski, J. Liigand, L. Zhang, J. Zheng, R. Mandal,

N. Karu, M. Dambrova, H. B. Schiöth, R. Greiner and V. Gautam, *Nucleic Acids Res.*, 2022, **50**, D622–D631.
20 M. R. Molenaar, A. Jeucken, T. A. Wassenaar, C. H. A. van de Lest, J. F. Brouwers and J. B. Helms, *Gigascience*, 2019, **8**(6), DOI: 10.1093/gigascience/giz061.
21 S. Trefely, K. Huber, J. Liu, M. Noji, S. Stransky, J. Singh, M. T. Doan, C. D. Lovell, E. von Krusenstiern, H. Jiang, A. Bostwick, H. L. Pepper, L. Izzo, S. Zhao, J. P. Xu, K. C. Bedi, J. E. Rame, J. G. Bogner-Strauss, C. Mesaros, S. Sidoli, K. E. Wellen and N. W. Snyder, *Mol. Cell*, 2022, **82**, 447–462.
22 S. Vinga, A. R. Neves, H. Santos, B. W. Brandt and S. A. L. M. Kooijman, *Philos. Trans. R. Soc., B*, 2010, **365**, 3429–3442.
23 D. Wevers, R. Ramautar, C. Clark, T. Hankemeier and A. Ali, *Electrophoresis*, 2023, **44**, 2000–2024.
24 J. Wahrheit and E. Heinzle, *Quenching methods for the analysis of intracellular metabolites*, 2014, pp. 211–221.
25 H. Du, T. Xu, S. Yu, S. Wu and J. Zhang, *Signal Transduction Targeted Ther.*, 2025, **10**, 245.
26 S.-H. Kim, Y.-S. Cho and Y.-K. Jung, *Exp. Mol. Med.*, 2025, **57**, 2418–2428.
27 A.-R. Remy, J. B. Ghrayche and E. J. New, *Redox Exp. Med.*, 2025, **2025**(1), DOI: 10.1530/REM-25-0005.
28 P. V. S. Oliveira, T. C. De Bessa and F. R. M. Laurindo, *Biochemistry*, 2026, **65**, 1–30.
29 A. Vercaemst, M. Zhao, R. Chai, C. Lismont and M. Fransen, *Cells*, 2026, **15**, 254.
30 A. Schmidt, M. Pfeiffer and S. Sdelci, *npj Metab. Health Dis.*, 2026, **4**, 6.
31 G. Lu, S. Xu, P. Huang and L. Li, *Proteomics*, 2026, **26**, 7–22.
32 R. J. Webb, J. K. Lodge, S. S. Scott and I. G. Davies, *Metabolites*, 2025, **15**, 68.
33 A. Jain and R. Zoncu, *Mol. Metab.*, 2022, **60**, 101481.
34 M. Abu-Remaileh, G. A. Wyant, C. Kim, N. N. Laqtom, M. Abbasi, S. H. Chan, E. Freinkman and D. M. Sabatini, *Science*, 2017, **358**, 807–813.
35 J. A. Olzmann and P. Carvalho, *Nat. Rev. Mol. Cell Biol.*, 2019, **20**, 137–155.
36 C. P. Najt, S. Adhikari, T. D. Heden, W. Cui, E. R. Gansemer, A. J. Rauckhorst, T. W. Markowski, L. Higgins, E. W. Kerr, M. D. Boyum, J. Alvarez, S. Brunko, D. Mehra, E. M. Puchner, E. B. Taylor and D. G. Mashek, *Cell Rep.*, 2023, **42**, 112435.
37 L. Scorrano, M. A. De Matteis, S. Emr, F. Giordano, G. Hajnóczky, B. Kornmann, L. L. Lackner, T. P. Levine, L. Pellegrini, K. Reinisch, R. Rizzuto, T. Simmen, H. Stenmark, C. Ungermann and M. Schuldiner, *Nat. Commun.*, 2019, **10**, 1287.
38 V. Pareek, Z. Sha, J. He, N. S. Wingreen and S. J. Benkovic, *Mol. Cell*, 2021, **81**, 3775–3785.
39 K. Wheeler, C. Gosmanov, M. Jimenez Sandoval, Z. Yang and L.-I. McCall, *TrAC, Trends Anal. Chem.*, 2024, **175**, 117713.
40 K.-J. Dietz, *J. Exp. Bot.*, 2017, **68**, 5695–5698.
41 K. E. Wellen and N. W. Snyder, *Curr. Opin. Clin. Nutr. Metab. Care*, 2019, **22**, 347–354.
42 M. J. Sarmento, A. Llorente, T. Petan, D. Khnykin, I. Popa, M. Nikolac Perkovic, M. Konjevod and M. Jaganjac, *Cell. Mol. Life Sci.*, 2023, **80**, 237.
43 R. Zhao, L. Zhang, S. Dong, K. Kamachi, S. K. Gupta, H. Akiyama, J. Nguyen, G. L. Hackman, M. Andreeff, A. Lodi and J. Ishizawa, *STAR Protoc.*, 2025, **6**, 104257.
44 S. Qin, M. Gao, Q. Zhang, Q. Xiao, J. Fu, Y. Tian, Y. Jiao, Z. Zhang, P. Zhang and F. Xu, *Anal. Chem.*, 2023, **95**, 10034–10043.
45 A. L. de Jager, S. Kassem, L. Alesha, B. A. E. Naber, I. F. de Laat, B. de Mooij, K. van der Pan, E. Bos, R. I. Koning, J. J. M. van Dongen, C. Teodosio and P. Díez, *Anal. Chem.*, 2026, **98**, 4585–4600.
46 D. F. Bodenstein, P. Powlowski, K. A. Zachos, D. El Soufi El Sabbagh, H. Jeong, L. Attisano, L. Edgar, D. C. Wallace and A. C. Andreazza, *Stem Cell Res. Ther.*, 2023, **14**, 202.
47 V. Skalický, I. Antoniadi, K. Ljung and O. Novák, *J. Exp. Bot.*, 2025, **77**, 120–133.
48 A. K. Tharkeshwar, D. Demedts and W. Annaert, *STAR Protoc.*, 2020, **1**, 100122.
49 V. Bhushan and A. Nita-Lazar, *J. Proteome Res.*, 2024, **23**, 2700–2722.
50 M. Leiro, R. Ventura, N. Rojo-Querol and M. Hernández-Alvarez, *Bio. Protoc.*, 2023, **13**(17), e4803, DOI: 10.21769/BioProtoc.4803.
51 J. Reinhard, L. Starke, C. Klose, P. Haberkant, H. Hammarén, F. Stein, O. Klein, C. Berhorst, H. Stumpf, J. P. Sáenz, J. Hub, M. Schuldiner and R. Ernst, *EMBO J.*, 2024, **43**, 1653–1685.
52 E. Yifrach, D. Holbrook-Smith, J. Bürgi, A. Othman, M. Eisenstein, C. W. van Roermund, W. Visser, A. Tirosh, M. Rudowitz, C. Bibi, S. Galor, U. Weill, A. Fadel, Y. Peleg, R. Erdmann, H. R. Waterham, R. J. A. Wanders, M. Wilmanns, N. Zamboni, M. Schuldiner and E. Zalckvar, *Mol. Syst. Biol.*, 2022, **18**(9), e11186.
53 X. Chen and Y. Wang, *Quantitave Proteomics Analysis of Purified Rat Liver Golgi*. 2023, pp. 417–430.
54 E. Zarate, V. Boyle, U. Rupprecht, S. Green, S. Villas-Boas, P. Baker and F. Pinu, *Metabolites*, 2016, **7**, 1.
55 N. Frolova, A. Orlova, V. Popova, T. Bilova and A. Frolov, *Biomolecules*, 2025, **16**, 16.
56 A. Diaz-Vegas, A. Don and J. Burchfield, *Bio. Protoc.*, 2024, **18**(9), e11186.
57 W. Qian, H. Tang and H. Yao, *J. Biol. Methods*, 2025, **12**, e99010049.
58 M. A. Brunet and M. L. Kraft, *Acc. Chem. Res.*, 2023, **56**, 752–762.
59 E. A. Bonnin and S. O. Rizzoli, *Front. Behav. Neurosci.*, 2020, **14**, 124.
60 E. A. Bonnin, A. Golmohammadi, R. Rehm, C. Tetzlaff and S. O. Rizzoli, *Life Sci. Alliance*, 2024, **7**, e202302030.
61 C. Lechene, F. Hillion, G. McMahon, D. Benson, A. M. Kleinfeld, J. P. Kampf, D. Distel, Y. Luyten, J. Bonventre, D. Hentschel, K. M. Park, S. Ito,

M. Schwartz, G. Benichou and G. Slodzian, *J. Biol.*, 2006, **5**, 20.
62 M. K. Passarelli, A. Pirkl, R. Moellers, D. Grinfeld, F. Kollmer, R. Havelund, C. F. Newman, P. S. Marshall, H. Arlinghaus, M. R. Alexander, A. West, S. Horning, E. Niehuis, A. Makarov, C. T. Dollery and I. S. Gilmore, *Nat. Methods*, 2017, **14**, 1175–1183.
63 V. Denti, G. Capitoli, I. Piga, F. Clerici, L. Pagani, L. Criscuolo, G. Bindi, L. Principi, C. Chinello, G. Paglia, F. Magni and A. Smith, *J. Proteome Res.*, 2022, **21**, 2798–2809.
64 M. A. Müller, N. Zweig, B. Spengler, M. Weinert and S. Heiles, *Anal. Chem.*, 2023, **95**, 11672–11679.
65 Z. Yin, X. Cheng, R. Liu, X. Li, L. Hang, W. Hang, J. Xu, X. Yan, J. Li and Z. Tian, *Angew. Chem., Int. Ed.*, 2019, **58**, 4541–4546.
66 H. Zhang, K. H. Lu, M. Ebbini, P. Huang, H. Lu and L. Li, *npj Imaging*, 2024, **2**, 20.
67 A. Potthoff, J. Schwenzfeier, M. Niehaus, S. Bessler, E. Hoffmann, O. Soehnlein, J. Höhndorf, K. Dreisewerd and J. Soltwisch, *Nat. Commun.*, 2025, **16**, 9129.
68 P. J. Horn, N. R. Ledbetter, C. N. James, W. D. Hoffman, C. R. Case, G. F. Verbeck and K. D. Chapman, *J. Biol. Chem.*, 2011, **286**, 3298–3306.
69 P. J. Horn and K. D. Chapman, *Plant Signaling Behav.*, 2011, **6**, 1594–1596.
70 J. P. Schessner, V. Albrecht, A. K. Davies, P. Sinitcyn and G. H. H. Borner, *Nat. Commun.*, 2023, **14**, 5252.
71 M. S. Phelps, D. Sturtevant, K. D. Chapman and G. F. Verbeck, *J. Am. Soc. Mass Spectrom.*, 2016, **27**, 187–193.
72 A. Lita, A. N. Kuzmin, A. Pliss, A. Baev, A. Rzhevskii, M. R. Gilbert, M. Larion and P. N. Prasad, *Anal. Chem.*, 2019, **91**, 11380–11387.
73 C. Thiele and J. Spandl, *Curr. Opin. Cell Biol.*, 2008, **20**, 378–385.
74 T. Harayama and B. Antonny, *Cold Spring Harbor Perspect. Biol.*, 2023, **15**, a041409.
75 W. Lu, X. Su, M. S. Klein, I. A. Lewis, O. Fiehn and J. D. Rabinowitz, *Annu. Rev. Biochem.*, 2017, **86**, 277–304.
76 S. Arrivault, M. Guenther, A. Florian, B. Encke, R. Feil, D. Vosloh, J. E. Lunn, R. Sulpice, A. R. Fernie, M. Stitt and W. X. Schulze, *Mol. Cell. Proteomics*, 2014, **13**, 2246–2259.
77 J. Aldana, A. Romero-Otero and M. P. Cala, *Metabolites*, 2020, **10**, 231.
78 C. Tabasso, C. K. Gavini, K. Z. Berry, H. Salem, A. Aguettaz, S. Lagarrigue, B. C. Bergman, V. Mansuy-Aubert and F. Amati, *BioRXiv preprint*, 2025, 10.64898/2025.12.24.696434.
79 H. Sedighikamal and S. Mashayekhan, *Metabolomics*, 2025, **21**, 40.
80 Y. Gao, Z. Xiong and X. Wei, *Metabolites*, 2025, **15**, 513.
81 H.-W. Liao, Y.-W. Cheng, S.-C. Tang and C.-H. Kuo, *J. Pharm. Biomed. Anal.*, 2022, **219**, 114930.
82 T. H. More and K. Hiller, *Curr. Opin. Biotechnol.*, 2022, **75**, 102711.
83 Z. Wang, H. Zhu and W. Xiong, *Sci. Bull.*, 2023, **68**, 2268–2284.
84 L. J. Foster, C. L. de Hoog, Y. Zhang, Y. Zhang, X. Xie, V. K. Mootha and M. Mann, *Cell*, 2006, **125**, 187–199.
85 J. A. Christopher, C. Stadler, C. E. Martin, M. Morgenstern, Y. Pan, C. N. Betsinger, D. G. Rattray, D. Mahdessian, A.-C. Gingras, B. Warscheid, J. Lehtiö, I. M. Cristea, L. J. Foster, A. Emili and K. S. Lilley, *Nat. Rev. Methods Primers*, 2021, **1**, 32.
86 H. T. Parsons and J. L. Heazlewood, *Front. Plant Sci.*, 2015, **6**, 301.
87 Y. Li, M. Bouza, C. Wu, H. Guo, D. Huang, G. Doron, J. S. Temenoff, A. A. Stecenko, Z. L. Wang and F. M. Fernández, *Nat. Commun.*, 2020, **11**, 5625.
88 C. Y. Tseng, J. A. Salguero, J. D. Breidenbach, E. Solomon, C. K. Sanders, T. Harvey, M. G. Thornhill, S. J. Palmisano, Z. J. Sasiene, B. R. Blackwell, E. M. McBride, K. A. Luchini, E. S. LeBrun, M. Alvarez, P. M. Mach, E. S. Rivera and T. G. Glaros, *Metabolomics*, 2025, **21**, 98.
89 S. Wije Munige, D. Bhusal, Z. Peng, D. Chen and Z. Yang, *JACS Au*, 2025, **5**, 2379–2387.
90 Y. Gong and S. Weinberg, *Biomolecules*, 2025, **15**, 1687.
91 M. Y. Hein, D. Peng, V. Todorova, F. McCarthy, K. Kim, C. Liu, L. Savy, C. Januel, R. Baltazar-Nunez, M. Sekhar, S. Vaid, S. Bax, M. Vangipuram, J. Burgess, L. Njoya, E. Wang, I. E. Ivanov, J. R. Byrum, S. Pradeep, C. G. Gonzalez, Y. Aniseia, J. S. Creery, A. H. McMorrow, S. Sunshine, S. Yeung-Levy, B. C. DeFelice, S. B. Mehta, D. N. Itzhak, J. E. Elias and M. D. Leonetti, *Cell*, 2025, **188**, 1137–1155.
92 C. Jang, L. Chen and J. D. Rabinowitz, *Cell*, 2018, **173**, 822–837.
93 W. W. Chen, E. Freinkman, T. Wang, K. Birsoy and D. M. Sabatini, *Cell*, 2016, **166**, 1324–1337.
94 B. Moiz, A. Li, S. Padmanabhan, G. Sriram and A. M. Clyne, *Metabolites*, 2022, **12**, 1066.
95 W. Dong, E. S. Rawat, G. Stephanopoulos and M. Abu-Remaileh, *Curr. Opin. Biotechnol.*, 2022, **76**, 102739.
96 T. Fuhrer and N. Zamboni, *Curr. Opin. Biotechnol.*, 2015, **31**, 73–78.
97 J. R. Kraly, R. E. Holcomb, Q. Guan and C. S. Henry, *Anal. Chim. Acta*, 2009, **653**, 23–35.
98 D. N. Itzhak, S. Tyanova, J. Cox and G. H. Borner, *eLife*, 2016, **9**(5), e16950.
99 A. Geladaki, N. Kočevar Britovšek, L. M. Breckels, T. S. Smith, O. L. Vennard, C. M. Mulvey, O. M. Crook, L. Gatto and K. S. Lilley, *Nat. Commun.*, 2019, **10**, 331.
100 A. Christoforou, C. M. Mulvey, L. M. Breckels, A. Geladaki, T. Hurrell, P. C. Hayward, T. Naake, L. Gatto, R. Viner, A. M. Arias and K. S. Lilley, *Nat. Commun.*, 2016, **7**, 9992.
101 J. Kang, L. David, Y. Li, J. Cang and S. Chen, *Front. Genet.*, 2021, **12**, 635971.
102 Y. Hasin, M. Seldin and A. Lusis, *Genome Biol.*, 2017, **18**, 83.
103 P. G. Schiro, J. C. Gadd, G. S. Yen and D. T. Chiu, *J. Phys. Chem. B*, 2012, **116**, 10490–10495.

104 M. K. Passarelli, A. G. Ewing and N. Winograd, *Anal. Chem.*, 2013, **85**, 2231–2238.
105 M. L. Steinhauser and C. P. Lechene, *Semin. Cell Dev. Biol.*, 2013, **24**, 661–667.
106 M. Kompauer, S. Heiles and B. Spengler, *Nat. Methods*, 2017, **14**, 90–96.
107 R. Zenobi, *Science*, 2013, **3642**, 1243259.
108 J. J. Almagro Armenteros, C. K. Sønderby, S. K. Sønderby, H. Nielsen and O. Winther, *Bioinformatics*, 2017, **33**, 3387–3395.
109 C. E. Lawson, J. M. Martí, T. Radivojevic, S. V. R. Jonnalagadda, R. Gentz, N. J. Hillson, S. Peisert, J. Kim, B. A. Simmons, C. J. Petzold, S. W. Singer, A. Mukhopadhyay, D. Tanjore, J. G. Dunn and H. Garcia Martin, *Metab. Eng.*, 2021, **63**, 34–60.
110 Z. Cai, R. C. Poulos, J. Liu and Q. Zhong, *iScience*, 2022, **25**, 103798.
111 R. Argelaguet, A. S. E. Cuomo, O. Stegle and J. C. Marioni, *Nat. Biotechnol.*, 2021, **39**, 1202–1215.

